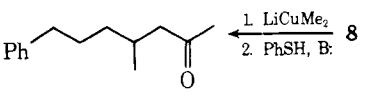

65%

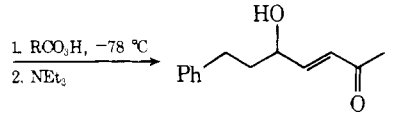

71%

sulfide, followed by oxidation gives the stable sulfoxide **9**. The methyl derivative was chosen to avoid the thio-Claisen rearrangements which occur (at 80 °C) with phenyl propargyl sulfoxide.[11] Compound **9** decomposes near 100 °C in the presence of $(MeO)_3P$ to give ill-defined mixtures, but no aldehyde. In the presence of triethylamine at 80 °C, allene **10** is formed in low yield.

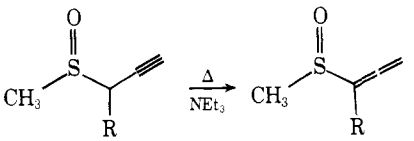

9, R = n-C_6H_{13} **10**

The dramatic lowering of the [2,3]sigmatropic shift activation energy in the selenium as compared to the sulfur analogue has resulted in interesting and useful chemistry of the selenium system not presently known for the sulfur analogues. The difference in behavior of propargyl selenoxides and sulfoxides is probably a consequence of the greater stability of selenenate vs. selenoxide[2b,9] (sulfoxides are usually more stable than sulfenates).

Acknowledgment. We thank the National Science Foundation for support of this work.

References and Notes

(1) (a) S. Hoff, L. Brandsma, and J. F. Arens, *Recl. Trav. Chim. Pays-Bas*, **87**, 916 (1968); (b) Y. Leroux and C. Roman, *Tetrahedron Lett.*, 2585 (1973); (c) R. M. Carlson, R. W. Jones, and A. S. Hatcher, *ibid.*, 1741 (1975); (d) F. Mercier, N. LeGoff, and R. Epsztein, *C.R. Acad. Sci., Ser. C*, **279**, 525 (1974); (e) B. W. Metcalf and P. Casara, *Tetrahedron Lett.*, 3337 (1975); (f) M. Huche and P. Cresson, *ibid.*, 367 (1975).

(2) Other selenium stabilized lithium reagents have been developed as synthetic reagents: (a) H. J. Reich and S. K. Shah, *J. Am. Chem. Soc.*, **97**, 3250 (1975); (b) H. J. Reich, *J. Org. Chem.*, **40**, 2570 (1975); (c) H. J. Reich and F. Chow, *J. Chem. Soc., Chem. Commun.*, 790 (1975); (d) K. B. Sharpless, R. F. Lauer, and A. Y. Teranishi, *J. Am. Chem. Soc.*, **95**, 6137 (1973); (e) D. Seebach and A. K. Beck, *Angew. Chem., Int. Ed. Engl.*, **13**, 806 (1974); (f) W. Dumont, P. Bayet, and A. Krief, *ibid.*, **13**, 804 (1974); J. N. Denis, W. Dumont, and A. Krief, *Tetrahedron Lett.*, 453 (1976); (g) R. H. Mitchell, *J. Chem. Soc., Chem. Commun.*, 990 (1975).

(3) Polylithium reagents derived from propyne and phenylpropyne have been previously prepared: (a) J. Klein and S. Brenner, *Tetrahedron*, **26**, 2345 (1970); *J. Org. Chem.*, **36**, 1319 (1971); (b) T. L. Chwang and R. West, *J. Am. Chem. Soc.*, **95**, 3324 (1973); (c) L. Brandsma and E. Mugge, *Recl. Trav. Chim. Pays-Bas*, **92**, 628 (1973); (d) N. M. Libman, V. I. Zlobina, and S. G. Kuznetsov, *Zh. Org. Khim.*, **10**, 2057 (1974); (e) F. Scheinmann et al., *J. Chem. Soc., Chem. Commun.*, 1030 (1974), 817 (1975).

(4) Among the systems tried, a significant amount of selenoxide syn elimination occurs only for **3a**, R = $PhCH_2$, E = Me_3SiCl (38% yield of 1-phenyl-4-trimethylsilylbut-1-ene-3-yne).

(5) Good yields of selenoenone **5a** are obtained when **3a** is oxidized at −78 °C (30 min) with *m*-chloroperbenzoic acid in dichloromethane, 1.5 equiv of pyridine is added, and the reaction mixture is warmed to 0 °C. A mixture of *E* and *Z* isomers is formed, equilibration to *Z* occurs on stirring at room temperature in the presence of pyridine.

(6) For example, warming **3b** (R = $(CH_2)_3Ph$, X = H) in the presence of $HNEt_2$, H_2NiBu, $P(OCH_3)_3$, MeOH, EtOH, HOAc, PhSH/Py, n-$Bu_4N^+I^-$, and I_2 did not give useful yields of **5b**.

(7) The *m*-trifluoromethyl substituted selenoxide isomerizes 0.84 times as fast as the unsubstituted compound ($k_{CF_3} = (9.0 \pm 0.5) \times 10^{-5}$ at −31 °C).

(8) A related selenenylation reaction has been found to give selenium containing by-products during the formation of enones by selenoxide syn elimination: H. J. Reich, J. M. Renga, and I. L. Reich, *J. Am. Chem. Soc.*, **97**, 5434 (1975).

(9) [2,3]Sigmatropic rearrangements of allyl selenoxides occur readily:[2b,d] K. B. Sharpless and R. F. Lauer, *J. Am. Chem. Soc.*, **95**, 2697 (1973); *J. Org. Chem.*, **37**, 3973 (1972).

(10) W. Kreiser and H. Wurziger, *Tetrahedron Lett.*, 1669 (1975).

(11) K. C. Majumdar and B. S. Thyagarajan, *J. Chem. Soc., Chem. Commun.*, 83 (1972); Y. Makisumi and S. Takada, *ibid.*, 848 (1974).

(12) Alfred P. Sloan Fellow, 1975–1977.

Hans J. Reich,*[12] Shrenik K. Shah

Department of Chemistry, University of Wisconsin
Madison, Wisconsin 53706

Received July 15, 1976

Electron Density Distribution of the Azide Ion. Quantitative Comparison of Theoretical Calculations with Experimental Measurements

Sir:

Recent progress in the experimental determination of electron density distributions in solids by x-ray (and neutron) diffraction[1] has generated renewed interest in theoretical calculation of the density distribution and in comparison with experiment.[2] Until now, the experimental difficulties in making measurements on small molecules, for which good theoretical calculations are available, and the computational difficulties in treating larger systems, for which experimental densities have been determined, have prevented comparisons between theory and experiment on the same system. Reported here is a quantitative comparison of the experimental electron density distributions in crystals of NaN_3 and KN_3 with a thermally smeared theoretical density of the azide ion.

The details of the electron density distribution are best visualized in a plot of the deformation density, $\Delta\rho$, given by the difference between the observed density and the density of an assembly of spherical atoms placed at the atomic positions. Values for the atomic positions and thermal vibration parameters unbiased by the valence electron distribution are required. These have been obtained by independent neutron diffraction experiments[3] ($\Delta\rho$ (X–N)) and by refinement of high order x-ray data ($\Delta\rho$ (X–X)).

The distribution of errors in the experimental deformation densities has been calculated as described by Rees[4] considering the contributions from errors in the x-ray intensity measurements, in the refined parameters, and in the x-ray scale factor. Assuming the contributions to be uncorrelated,

$$\sigma^2(\Delta\rho) = \sigma^2(\rho_{obsd}) + \sigma^2(\rho_{calcd}) + \rho_{obsd}{}^2\sigma^2(k)/k^2$$

where k is the x-ray scale factor. While the first contribution is relatively constant throughout the crystal (except near symmetry elements), the second and third contributions peak at the atomic centers, and differences between densities within about 0.3 Å of the nuclear positions cannot be considered significant.

Sodium azide crystallizes in space group $R\bar{3}m$ with the N_3^- ion on a crystallographic $\bar{3}m$ site. X-ray intensity measurements were collected from a single crystal on a Picker card-controlled diffractometer with graphite-monochromatized Mo Kα radiation.[5] Anharmonic (third cumulant[6]) thermal parameters were included in a full-matrix least-squares refinement of the structure. Refinement of 139 high order reflections ($0.65 < \sin\theta/\lambda < 1.25$ Å^{-1}) gave $R = 2.6\%$ and $R_w = 1.7\%$.[7] The $\Delta\rho$ (X–X) deformation density was calculated using the full data set (208 reflections with $0.0 < \sin\theta/\lambda < 1.25$ Å^{-1}), positional and thermal parameters from the high order refinement, and Hartree–Fock atomic scattering factors.[8] The x-ray scale factor was determined by experimental measurement.[9]

Potassium azide crystallizes in space group $I4/mcm$ with the N_3^- ion occupying a site with mmm symmetry. Single-crystal x-ray intensity measurements were collected on a Picker FACS-I diffractometer using Nb-filtered Mo Kα radiation. A total of 3463 reflections were measured in the range $0 < \sin$

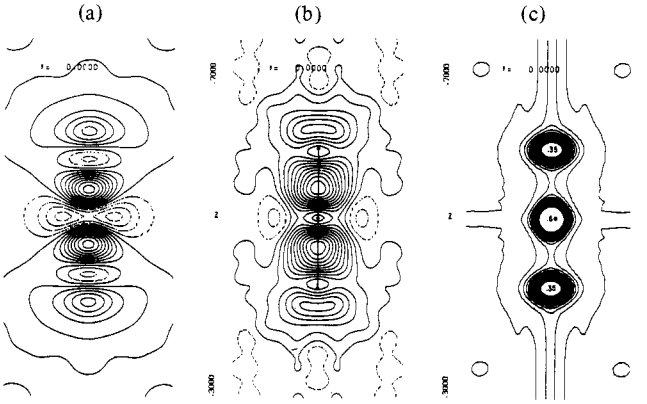

Figure 1. Deformation density of the azide ion with thermal motion as in NaN_3: (a) theoretical density, contours at 0.05 e/Å^3, negative contours broken; (b) experimental density, contours at 0.05 e/Å^3, atomic positions and molecular axis are indicated; (c) Error distribution in experimental deformation density, contours at 0.015 e/Å^3, lowest contour is 0.015 e/Å^3, highest contours omitted and labeled within maximum values.

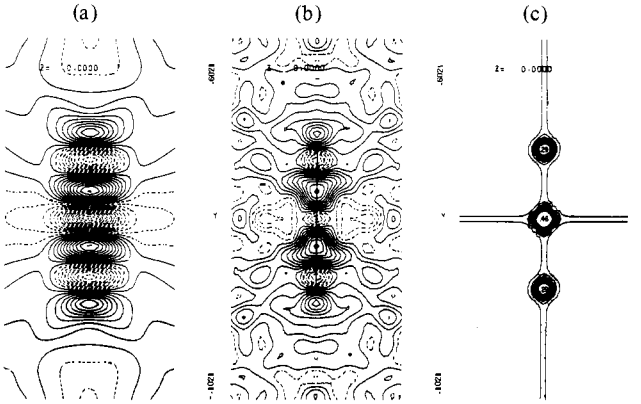

Figure 2. Deformation density of the azide ion with thermal motion as in KN_3. Contours as given for Figure 1: (a) theoretical density; (b) experimental density; (c) error distribution, lowest contour is 0.045 e/Å^3.

$\theta/\lambda < 1.25$ Å^{-1}, yielding 511 independent reflections. Refinement of 366 high order reflections ($\sin\theta/\lambda > 0.75$ Å^{-1}) gave $R = 6.6\%$ and $R_w = 2.2\%$. The $\Delta\rho$ (X–X) density for KN_3 was calculated using the full data set and parameters from the high order x-ray refinement. The scale factor was determined by least-squares refinement with all other parameters fixed.

The theoretical deformation density of the azide ion was obtained from an ab initio SCF molecular orbital calculation using the program HONDO[10] and an extended basis set of Gaussian orbitals. Experience has shown that the density distribution is highly sensitive to the quality of the wave function, and considerably larger than minimal basis set calculations are required to obtain reliable theoretical densities.[2] A set of 11s, 5p, 1d primitive Gaussians was contracted to five sets of s, three sets of p, and one set of d type orbitals on each nitrogen.

To minimize the effects of the basis set, the theoretical difference density was obtained by subtracting atomic densities calculated using the same basis set. Such spherical densities for nitrogen were obtained in a closed shell calculation with half occupancy assigned to the p orbitals.

Since the experimental densities represent a time average over the thermal motions of the molecule, thermal smearing has been applied to the theoretical densities for comparison. Molecular scattering factors corresponding to each experimental measurement were calculated by Fourier transformation of the wave function. Then a temperature factor was applied, and the smeared density obtained by an inverse Fourier transformation. The temperature factor included both translational and librational terms corresponding to the rigid body thermal motion found experimentally for each of the crystal structures. In this manner, in addition to thermal smearing, the effects of finite resolution (due to the finite number of terms in the Fourier series) are included in the theoretical as well as the experimental densities. Dynamic densities have been calculated for thiourea by a similar procedure.[11] When Hartree–Fock atomic densities are subtracted rather than atomic densities calculated with the extended basis set, the theoretical difference density is lower by about 0.15 e/Å^3 near the nuclear positions and higher by about 0.04 e/Å^3 in the bonds and lone pairs.

In Figure 1, the theoretical deformation density of the azide ion is compared with the experimental $\Delta\rho$ (X–X) density of NaN_3. Also included is the distribution map of the estimated standard deviation in the experimental deformation density. Note the difference in contour levels in the error map.

The significant features of the deformation density are large peaks in the N–N bonding regions and peaks at each end of the molecule commonly associated with lone pair density on the end nitrogens. The experimental peak heights are 0.52 and 0.23 e/Å^3 with estimated standard deviations of 0.05 and 0.03 e/Å^3 for the bond and lone pair peaks, respectively. The corresponding peak heights of the thermally smeared theoretical density are 0.44 and 0.26 e/Å^3. Comparison of the dimensions (width at half-height) of the bond and lone pair densities is good except for the bond peak which is more extended in the direction of the molecular axis in the experimental density. Sections perpendicular to the molecular axis through the bond and lone pair peaks show these features to be very nearly cylindrically symmetric.

In Figure 2, the theoretical and experimental ($\Delta\rho$ (X–X)) deformation densities and error distribution are plotted for KN_3. The experimental peak heights are found to be 0.46 and 0.37 e/Å^3 with standard deviations of 0.06 and 0.05 e/Å^3 in the bond and lone pair regions. The corresponding peak heights of the thermally smeared theoretical density are 0.55 and 0.40 e/Å^3, respectively. The shape of experimental bond and lone pair peaks are again in good agreement with the theoretical results except for the width of the lone pair peak which is considerably more extended perpendicular to the molecule in the theoretical density. As in NaN_3, the experimental bond peak is more extended along the molecule axis.

Except in the areas noted, the overall agreement between theory and experiment is excellent (within $\sim 2\sigma(\Delta\rho)$) in both NaN_3 and KN_3. Although the theoretical results may suffer somewhat from the neglect of crystal forces in the calculation and internal vibrations in the smearing, the remaining discrepancies are more likely due to basis set truncation and neglect of electron correlation in the theoretical maps. Comparison of the unsmeared N_3^- theoretical density with the Hartree–Fock density for N_2[12] suggests that even the extended basis set employed here may be deficient in the bonding region, and account for the lack of extension along the molecule of the theoretical bond peaks.

A recent calculation of the density corresponding to a CI wave function of N_2,[13] gives a maximum increase of 0.13 e/Å^3 relative to the HF density. The maximum in the CI–HF difference density is located near the nitrogen but displaced $\sim$0.3 Å off the molecular axis. Such a discrepancy between HF and CI densities, if confirmed by further calculations, would account for the higher experimental density found in those regions, giving the bond peaks their somewhat square shape.

Although the experiment yields only the density and not the molecular wave function, it does provide a powerful criterion for judging theoretical calculations. In addition, with appropriate attention to experiment design and distribution of errors

in the result, densities may be determined for much larger systems of chemical interest.

Acknowledgment. Support of this work by the National Science Foundation is gratefully acknowledged.

References and Notes

(1) P. Coppens, *MTP Int. Rev. Sci., Phys. Chem. Ser.*, **11**, 21 (1975); P. Coppens and E. D. Stevens, *Adv. Quantum Chem.*, in press.
(2) R. F. W. Bader, *MTP Int. Rev. Sci., Phys. Chem. Ser.*, **1**, Butterworths, 43 (1975); P. E. Cade, *Trans. Am. Crystallogr. Assoc.*, **8**, 1–36 (1972).
(3) C. S. Choi, private communication.
(4) B. Rees, *Acta Crystallogr., Sect. A*, **32**, 483–488 (1976).
(5) E. D. Stevens, Thesis, University of California, Davis, 1973.
(6) C. K. Johnson, *Acta Crystallogr., Sect. A*, **25**, 187–194 (1969).
(7) $R = \Sigma(|F_{obsd}| - |F_{calcd}|)/\Sigma|F_{obsd}|$ and $R_w = (\Sigma w(|F_{obsd}| - |F_{calcd}|)^2/\Sigma w|F_{obsd}|^2)^{1/2}$ where $w = 1/\sigma^2(F_{obsd})$.
(8) P. A. Doyle and P. S. Turner, *Acta Crystallogr., Sect. A*, **24**, 390–397 (1968).
(9) E. D. Stevens and P. Coppens, *Acta Crystallogr., Sect. A*, **31**, 612–619 (1975).
(10) H. F. King and M. Dupuis, *J. Comput. Phys.*, **21**, 141 (1976). M. Dupuis, J. Rys, and H. F. King, *J. Chem. Phys.*, **65**, 111–116 (1976).
(11) H. L. Hase, H. Reitz, and A. Schweig, *Chem. Phys. Lett.*, **39**, 157–159 (1976).
(12) R. F. W. Bader, W. H. Henneker, and P. E. Cade, *J. Chem. Phys.*, **46**, 3341–3363 (1967).
(13) P. Becker, private communication; F. Grimaldi, A. Lecourt, and C. Moser, *Int. J. Quantum Chem.*, **1S**, 153 (1967).

E. D. Stevens,* J. Rys, P. Coppens*
Department of Chemistry
State University of New York at Buffalo
Buffalo, New York 14214
Received May 25, 1976

Methods for the Preparation of 1,5-Dienes. A Metathetical Route to Medium-Sized Carbocycles

Sir:

The development of methods for the synthesis of medium-sized carbocycles is stimulated by the occurrence of such moieties in multifarious natural products of biological interest. Important synthetic targets among such naturally occurring carbocycles include the germacradienes,[1] a sesquiterpene family characterized by a ten-membered ring nucleus **1.** Interest in the synthesis of compounds of this structural type arises, in part, from the reported in vivo activity[2] of various germacradienes against carcinosarcoma in rats and lymphocytic leukemia in mice and their further use in biogenetically modeled syntheses of other sesquiterpene skeletons.[3] In connection with these considerations, we wish to report the synthetic salience of a metathetical route (a) to medium-sized carbocycles following the strategy outlined in Scheme I. A variation (b) of this merged cycloaddition–retrocycloaddition sequence is also described which allows for the addition of differentiated vinyl groups across a carbon–carbon double bond.

The previously unreported photocycloaddition of methyl cyclobutenecarboxylate (**2**)[4] with cycloalkenes provided a convenient route to the tricyclic intermediates in the above sequence. For example, irradiation[5] (3 h) of a 0 °C degassed methylene chloride solution of ester **2** and cyclopentene afforded photoadduct **3**[6] (67% yield; IR (neat) 1725 cm^{-1}; NMR ($CDCl_3$) δ 3.66 (s, 3), 1.47–3.08 (m, 13)), which was initially used to evaluate the above strategy. When photoadduct **3** (0.2 M benzene, sealed Pyrex tube) was heated at 180 °C for 3 h, ester **4** was obtained in 70% yield along with unreacted starting material. The structure of **4** is indicated by its spectroscopic properties (IR (neat) 1730 cm^{-1}; NMR ($CDCl_3$) δ 6.17 (bs, 1), 4.69–5.70 (m, 3), 5.44 (bs, 1), 3.69 (s, 3), 2.72–3.23 (m, 2), and 1.33–2.22 (m, 6)) and conversion (O_3, HOAc/EtOAc, 0 °C; H_2O_2, 65 °C, 12 h) to *cis*-1,2-cyclopentanedicarboxylic acid (mp 135–136 °C).[7] The formation of ester **4,** in this instance, may be explained by kinetic cleavage (a) of photoadduct **3** or cleavage (b) followed by a Cope rearrangement.[8]

Scheme I

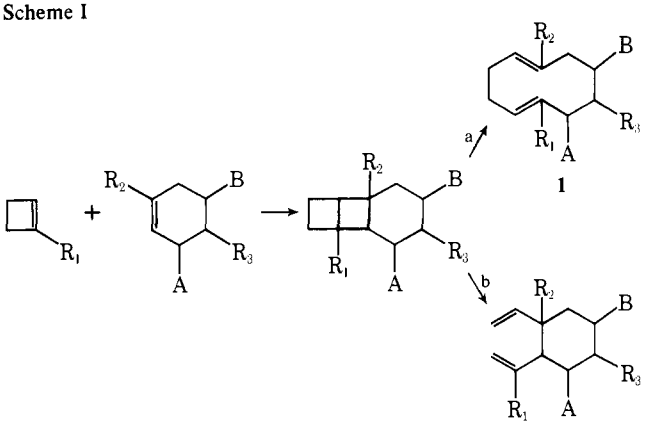

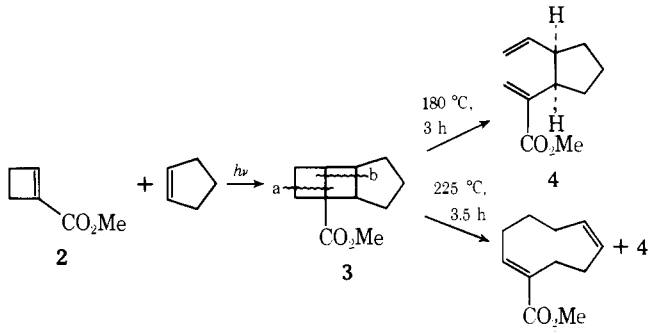

That the course of the above rearrangement and, hence, product formation can be subject to experimental control was demonstrated in a second pyrolysis experiment using photoadduct **3** (0.2 M benzene, 225 °C, 3.5 h). Under these conditions, cyclononadiene ester **5** and ester **4** (2:1 mixture) were obtained in a combined yield of 90%. The structure of **5** is assigned from its spectroscopic data (IR (neat) 1710 and 730 cm^{-1}; NMR ($CDCl_3$) δ 6.80 (t, 1, J = 9 Hz), 5.77 (dt, 1, J = 8 and 10.5 Hz), 5.42 (dt, 1, J = 8 and 10.5 Hz), 3.72 (s, 3), and 1.44–2.50 (m, 10)), conversion to cyclononanecarboxylic acid[9a] (anilide, mp 140–141 °C),[9b] and interconversion with ester **4.**[8] Since the same ratio of esters (**5**/**4** = 2/1) is obtained when ester **4** is subjected to the above pyrolysis conditions, product formation, in this case, is thermodynamically controlled.

This approach is readily extended to the cyclodecadiene system. Thus, irradiation (Pyrex filter)[5,10] of a 0 °C degassed methylene chloride solution of isophorone and ester **2** afforded ketoester **6** (85% yield based on ester **2**). The isomeric purity of this product is indicated by its homogeneity by thin-layer chromatography and the presence of only four methyl singlets in its NMR spectrum (partial NMR ($CDCl_3$) δ 3.54 (s, 3), 1.29 (s, 3), 1.01 (s, 3), 0.94 (s, 3)) and corresponding